Accepted Manuscript

Phase crossover in columnar tris-(1,3,4-oxadiazoles) with pendant quinoxalines

Kuan-Ting Lin, Chung K. Lai

PII: S0040-4020(16)31012-2

DOI: 10.1016/j.tet.2016.10.003

Reference: TET 28144

To appear in: *Tetrahedron*

Received Date: 20 August 2016

Revised Date: 1 October 2016

Accepted Date: 4 October 2016

Please cite this article as: Lin K-T, Lai CK, Phase crossover in columnar tris-(1,3,4-oxadiazoles) with pendant quinoxalines, *Tetrahedron* (2016), doi: 10.1016/j.tet.2016.10.003.

Phase crossover in columnar tris-(1,3,4-oxadiazoles) with pendant quinoxalines

Kuan–Ting Lin and Chung K. Lai

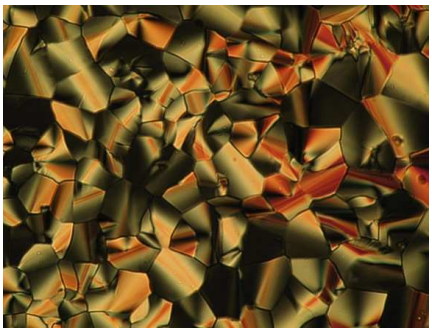

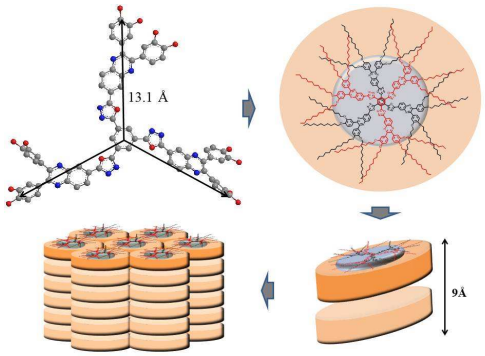

Phase crossover in columnar tris-(1,3,4-oxadiazoles) with pendant quinoxalines

Kuan–Ting Lin and Chung K. Lai
Department of Chemistry, National Central University
Chung–Li, Taiwan, ROC

Abstract. Four new series of bis–(1,3,4–oxadiazoles) **1a**–**c** and tris–(1,3,4–oxadiazoles) **1d** containing peripheral quinoxalines were prepared and their mesomorphic behavior was reported. Except for compound **1c** (n = 12), all other compounds **1a**–**d** formed columnar phases which were confirmed by powder X–ray diffractometer (XRD). Compounds **1d** have the highest clearing temperatures and the widest temperature range of columnar phases than those of other compounds **1a**–**b**. Compounds **1d** exhibited a phase crossover between the rectangular and hexagonal columnar phases. A value of N_{cell} = 2.85 and 2.16 Å within a column slice of 9.0 Å thick was obtained for compound **1a** (n = 12) and **1d** (n = 12), indicating that two molecule was correlated within columns in columnar phases. All compounds **1a**–**d** (n = 12) showed good stabilities at temperature below T_{dec} = 412.5–420.8 °C on thermogravimetric analysis. The PL spectra of all compounds **1a**–**d** (n = 12) showed one intense peak at λ_{max} = 517–520 nm, and these photoluminescent emissions originated from peripheral quinoxaline moiety.

*Corresponding author. Tel.: +886 03 4259207; fax: +886 03 4277972
e–Mail address: cklai@cc.ncu.edu.tw (C.K. Lai).

1.0 Introduction

1,3,4–Oxadiazole, as an important 5–membered ring heterocycle has been investigated in the field of materials chemistry due to their excellent thermal and chemical stabilities. Their potential applications have been fully reviewed.[1] 2,5–Diary–1,3,4–oxadiazoles[2] derivatives were well long known to show high photoluminescence quantum yields. Many studies have demonstrated their widespread uses as electron transporting/ hole blocking materials, emitting layers in electro–luminescent diodes, or for non–linear optical processes. 1,3,4–Oxadiazole is a nonlinear structure, stemming from its larger exocyclic bond angle[3] (~135°). Incorporating heteroatoms, such as nitrogen, oxygen, sulfur atoms might impact some chemical or physical properties, which were often not observed in their homologues all–carbon rings. Furthermore, these heteroatoms are more electronegative than carbons, and they all have delocalized lone electrons. These inherently molecular futures, such as electron unsaturation, electron–deficiency, nonplanar core, lower symmetries, higher polarizabilities or others often favorable for their induction or formation of the mesophases, have made them an excellent core in the design of mesogenic materials. The first mesogenic oxadiazoles[4] showing SmA and N phases were studied until 1993. A few examples columnar 1,3,4–oxadiazoles[5] and their metallomesogens[6] were previously reported by this group. In contrast, compounds containing bis– or tris–(1,3,4–oxadiazoles) (i.e. poly-1,3,4-oxadiazoles) were less prepared and studied. Known example of mesogenic bis–(1,3,4–oxadiazoles)[7] **Ia**–**b** or tris–(1,3,4–oxadiazoles)[8] **III** were very limited. Isomeric examples of mesogenic bis-(1,2,4-oxadiazoles)[9] were also explored.

Quinoxalines were also known as highly photoluminecent and/or efficient electroluminescent materials. Quinoxaline were highly π–conjugated fused backbones, and were useful in many applications[10] such as dyes, organic light-emitting diodes, electroluminescence, organic thin film transistors (TFT), and organic photovoltaics. They were considered as half–disc, elliptical or round molecules, which could easily or spontaneously self–assemble into columns when π–π interaction or dipole–dipole interactions are accessible in the solid or liquid crystalline states. These molecules capable of forming columnar stacking arrangements might have a dramatic

impact propensity. Examples of using bulky quinoxalines to improve mesomorphic behavior in 1,3,4–oxadiazole **IIa–b**[11] as core structure has been reported in our previous studies.

In this work, we report the preparation and mesomorphic studies of two new series of symmetrical bis–(1,3,4–oxadiazoles) **1a**–**c** and another series of tris–(1,3,4–oxadiazoles) **1d** in which a peripheral quinoxaline was incorporated to better induce their columnar phases. Interestingly, except for compounds **1c** (n = 12) all other compounds **1a**–**b** and **1d** formed columnar phases. Compound **1a f**ormed hexagonal columnar phase and compounds **1b** exhibited lamellar columnar phases. In contrast, all compounds **1d** (n = 8, 10, 12, 14) formed rectangular columnar at lower temperature and hexagonal columnar phase over a wide range of temperature. Their optical behavior was also studied.

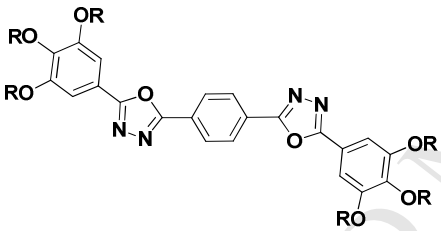

Ia; Col phase

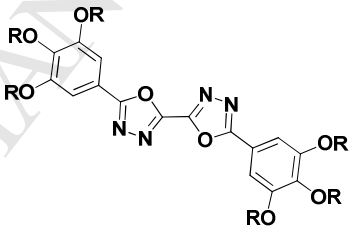

Ib; Col phase

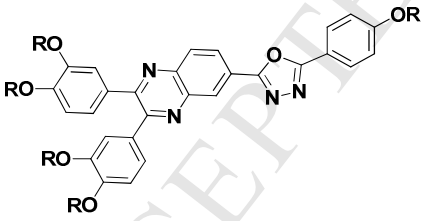

IIa; monotropic Col phase

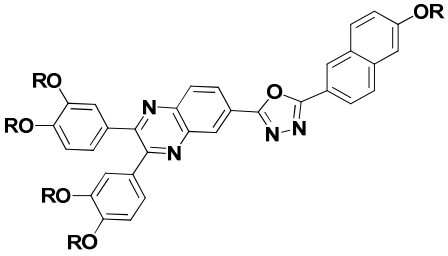

IIb; monotropic Col phase

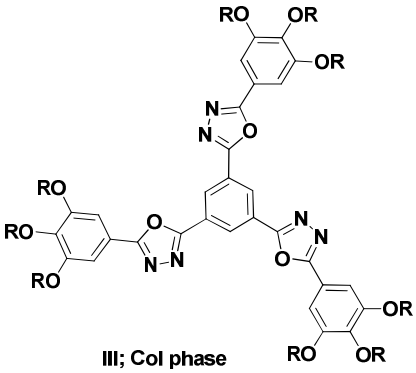

III; Col phase

2.0 Results and Discussion

2.1 Synthesis and characterization

The synthetic routes utilized to prepare bis-(1,3,4-oxadiazoles) **1a–c** and tris-(1,3,4-oxadiazoles) **1d** are listed in Scheme 1 and Scheme 2. The methyl 2,3–bis(3,4–bis (alkoxy)phenyl)quinoxaline 6–carboxylates **4**, isolated as yellow solids were similarly prepared by our previous procedures. Further reaction of methyl 6-carboxylates with hydrazine monohydrate in refluxing in THF/methanol gave yellowish 2,3–bis(3,4–bis(alkoxy)phenyl)quinoxaline–6–carbohydrazides **3**. A singlet peak appeared at ca. ~4.23 ppm on ^{1}H–NMR spectrum, assigned for –NH_2 confirmed its formation. Furthermore, the precursors **2a**–**c**, quinoxaline–6–carbonyl) oxalohydrazides were obtained by reaction of quinoxaline–6–carbohydrazides and oxalyl chloride in the presence of triethylamine at ice bath in stirring THF. The 6-carbohydrazides **3**, isolated as yellow–green solids were directly used for next reaction without any further purification. The final compounds **1a**, 5,5'–bis(2,3–bis(3,4–bis(alkoxy)phenyl) quinoxalin–6–yl)–2,2'–bi (1,3,4–oxadiazoles) were prepared by neat reactions of N'1,N'2–bis (2,3–bis(3,4–bis(alkoxy) phenyl)quinoxaline–6–carbonyl)oxalohydrazides in refluxing phosphoryl chloride. The products isolated as bright yellow to orange solids were obtained after silica gel chromatography eluting with hexane/ethyl acetate and recrystallization from THF/methanol. All other compounds **1b**–**c** were obtained by above procedures. Four derivatives **1d** (n = 8, 10, 12, 14) of tris–(1,3,4–oxadiazoles) were similarly prepared according to Scheme 2. All final compounds **1a**–**d** were characterized by ^{1}H NMR, ^{13}C NMR, mass, and elemental analysis.

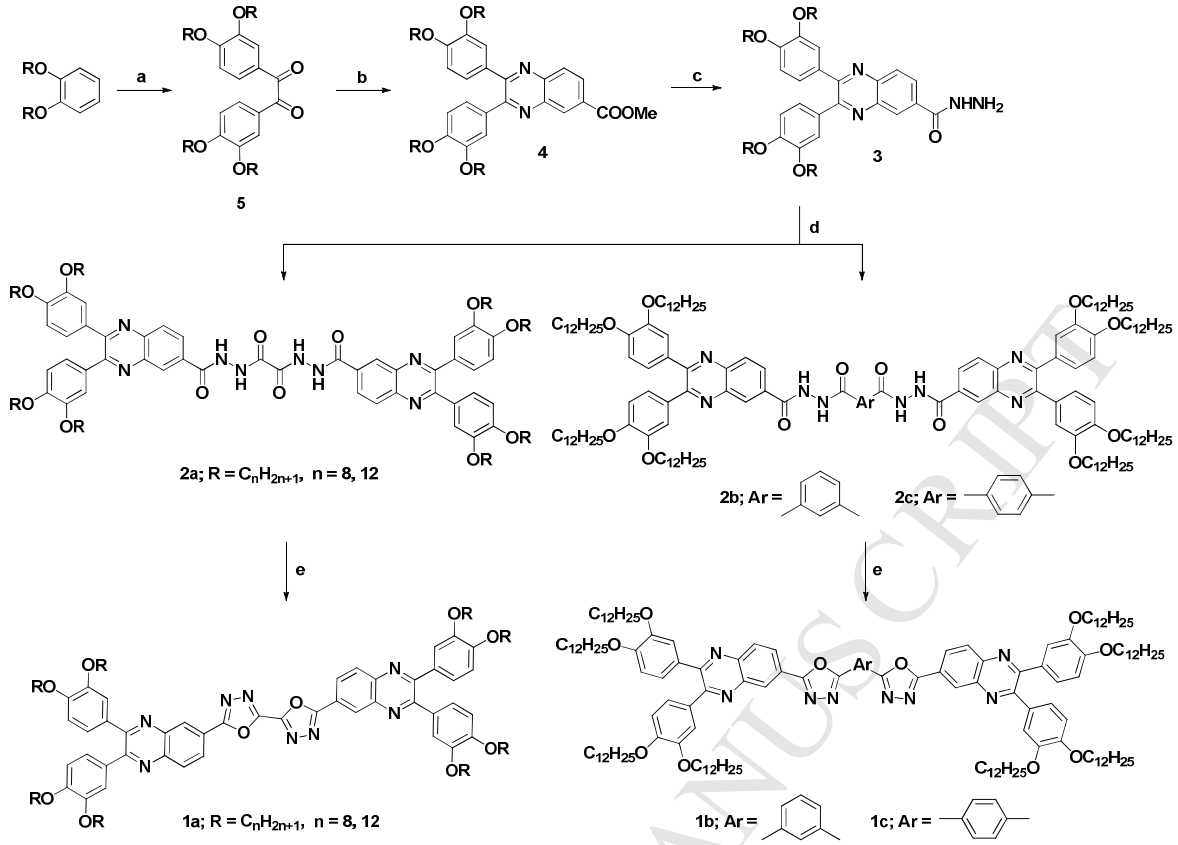

Scheme 1. Reagents and conditions: (a) $AlCl_3$, oxalyl chloride, stirring in CS_2 at 0°C for 6 h, 40-42%; (b) Methyl 3,4-diaminobenzoate, acetic acid, refluxing in THF for 24 h, 90-93%; (c) Hydrazine monohydrate, refluxing in THF and methanol for 12 h, 85-90%; (d) 1a, oxalyl dichloride, triethylamine, stirring in dry THF at rt. for 24 h; 1b, isophthaloyl dichloride, triethylamine, stirring in dry THF at rt. for 24 h; 1c, terephthaloyl dichloride, triethylamine, stirring in dry THF at rt. for 24 h; (e) refluxing in $POCl_3$ for 24 h, 25-43%.

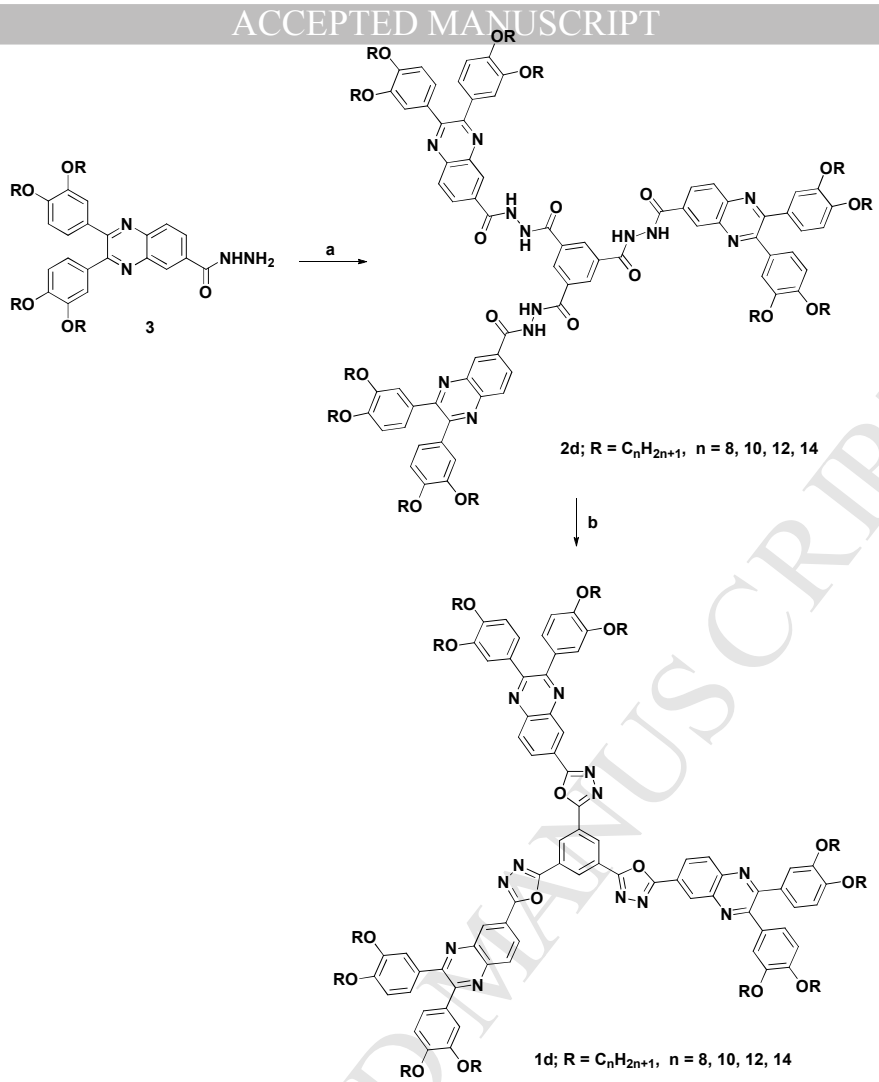

Scheme 2. Reagents and conditions: (a) benzene-1,3,5-tricarbonyl trichloride, triethylamine, stirring in dry THF at rt. for 24 h; (b) Refluxing in $POCl_3$ for 24 h, 35-40%.

2.2 Phase transitions, mesomorphic properties, and thermal stability of compounds 1a-d

The liquid crystalline behavior of compounds **1a–d** was characterized and studied by differential scanning calorimetry and polarized optical microscope. The phase transitions and thermodynamic data are summarized in Table 1. Except compounds **1c**, all three series of compounds **1a–b** and **1d** exhibited columnar mesomorphic behavior under POM observation (Fig. 1). Compound **1c** (n = 12) was not mesogenic, and only transition of crystal–to–isotropic at 158.7 °C with a large enthalpy of ΔH = 47.4 kJ/mol was observed on heating process. Both compound **1b** (n = 12) and **1c** (n = 12) were in fact molecular isomers. The lack of mesomorphism on compound **1c** (n = 12) might probably attributed to its overall molecular shape or/and molecular symmetry. Furthermore, its higher clearing temperature at 157.8 °C than that (T_{cl} = 117.3 °C) of

compound **1b** (n = 12) indicated that the intermolecular interaction in compound **1c** (n = 12) was indeed stronger than that in compound **1b** (n = 12). Interestingly, compound **1b** (n = 12) formed a lamella columnar phase (Col_L). DSC data showed that it clearing temperature at T_{cl} = 117.3 °C was observed on heating process, and its temperature was relatively short, ΔT_{Col} = 15.1 °C on cooling process. The shorter range of columnar phase indicated that the lamella columnar in such system is kinetically not very stable. Under optical microscope they exhibited typical focal–conic textures (Fig. 1), similar to hexagonal columnar textures, when cooled from its isotropic state. These optical textures also showed slightly small area of homeotropic domains which were commonly observed in columnar phases.

Fig. 1 Optical textures of columnar phases observed by compounds: **1a** (n = 12) at 122 °C (top left), **1b** (n = 12) at 105 °C (top right), **1d** (n = 8) at 166 °C (bottom left) and **1d** (n = 12) at 155 °C (bottom right).

In order to improve the induction of columnar phases in such discotic system derived from poly(1,3,4–oxadiazoles), four 1,3,4–oxadiazoles **1d** (n = 8, 10, 12, 14) with three pendant quinoxalines were prepared and their mesomorphic properties were investigated. As expected, all

tris−(1,3,4−oxadiazoles), as more rounded molecules formed better improved mesomorphic behavior. All compounds **1d** (n = 8, 10, 12, 14) exhibited a phase−crossover dependence on temperature; they formed rectangular columnar phases at lower temperature and hexagonal columnar phases at higher temperature. The phase crossover behavior between the Col_{rec} and Col_{hex} phases was enantiotropic. DSC data appeared that melting temperatures increased with carbon chain length; T_{mp} = 102.0 (n = 8) < 104.0 (n = 10) < 110.0 (n = 12) < 115.0 °C (n = 14) on heating process. In contrast, the clearing temperature decreased with carbon lengths; T_{cl} = 175.0 (n = 10) > 166.2 (n = 8) > 160.3 (n = 12) > 148.1 °C (n = 14) on heating process. Both enthalpies for the transition of Col_{rec}−to−Col_{hex} phase and Col_{hex}−to−I phase were relatively small; 0.60 (n = 8)−1.97 kJ/mol (n = 10) and 2.07 (n = 8)−5.25 kJ/mol (n = 14) on cooling process, respectively. This enthalpy dependence reflected macroscopically their molecular entropies when molecules changed from Col_{rec}-−to−Col_{hex}−to−I state. Under POM, a focal−conic or more leaf-like texture (Fig. 1) with linear birefringent defects was clearly observed when cooling from their isotropic liquids. These observed textures, accompanied by a larger area of homeotropic domain were characteristic for hexagonal columnar phases. The Figure 2 is the bar graphs showing the phase behavior of compounds **1a**−**d**

Table 1 The phase transitions and enthalpies[a] of compounds 1a-1d.

1a; n = 8			**Cr**	**118.8 (27.9)**	**Col_h**	**134.3 (41.4) 120.9 (9.56)**	**I**
n = 12			**Cr**	**113.6 (30.4) 104.5 (27.7)**	**Col_h**	**125.8 (8.17) 122.9 (8.36)**	**I**
1b; n = 12			**Cr**	**93.3[b] 90.8[b]**	**Col_L**	**117.3 (1.66) 105.9 (0.92)**	**I**
1c; n = 12					**Cr**	**157.8 (47.4) 142.6 (38.4)**	**I**
1d; n = 8	**Cr**	**102.0[b] 90.0[b]**	**Col_r**	**127.1 (1.78) 124.9 (1.97)**	**Col_h**	**175.0 (2.10) 167.6 (2.07)**	**I**
n = 10	**Cr**	**104.0[b] 95.0[b]**	**Col_r**	**132.8 (0.51) 130.7 (0.60)**	**Col_h**	**166.2 (2.94) 160.2 (2.64)**	**I**
n = 12	**Cr**	**110.0[b] 102.0[b]**	**Col_r**	**133.8 (0.47) 131.7 (0.63)**	**Col_h**	**160.3 (3.93) 155.9 (3.43)**	**I**
n = 14	**Cr**	**115.0[b] 103.0[b]**	**Col_r**	**129.1 (0.70) 127.2 (0.70)**	**Col_h**	**148.1 (5.28) 143.6 (5.25)**	**I**

[a]: n = the carbon number of alkoxy chains. Cr = crystal; Col_L = columnar lamellar phase; Col_r = columnar rectangular phase; Col_h = columnar hexaganol phase; I = isotropic phases.

[b]: observed by POM.

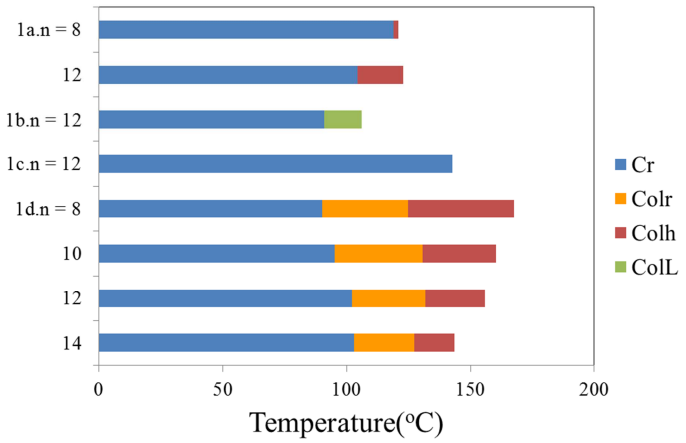

Fig. 2 Bar graphs showing the phase behavior of compounds **1a–d**. All temperatures were taken on the cooling process.

The thermal stability of compounds **1a–d** (all n = 12) was also performed by thermo-gravimetric analysis (TGA) under nitrogen atmosphere, shown in Fig. 3. All four compounds showed good thermal stability at temperature below ca. T_{dec} = 410 °C, with a relative thermal stability of **1b** > **1d** > **1a** > **1c**. The decomposition temperatures for a 5% weight loss were listed in Table 2.

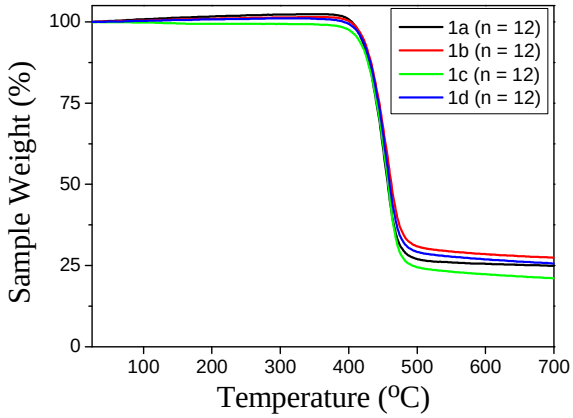

Fig. 3 The TGA thermographs of compounds **1a**–**d** (all n = 12) under nitrogen gas at a heating rate of 10.0 °Cmin^{-1}.

Table 2. The decomposition temperatures[a] of compounds **1a–d** measured by TGA analysis.

Compd.	T_{dec} (°C)
1a (n = 12)	417.5
1b (n = 12)	420.8
1c (n = 12)	412.5
1d (n = 12)	418.3

[a]: temperatures taken with a 5% weight loss under nitrogen atmosphere.

2.3 Powder X–ray diffractions of compounds 1a–b and 1d.

In order to confirm the structure of the columnar phases exhibited by compounds **1**, variable–temperature powder X–ray diffraction experiments of three compounds **1a**–**b** (n = 12) and **1d** (n = 12) were also conducted. Interestingly, compound **1a** (n = 12) formed hexagonal columnar phase, whereas, compound **1b** (n = 12) exhibited lamellar columnar phases. For the Col_h phase, a diffraction pattern of a two dimensional hexagonal lattice with one very strong diffraction peak at lower angle and another much weaker diffraction peak of compound **1a** (n = 12) was obtained at 120.0 °C under cooling process, shown in Fig. 4. A diffraction pattern with a *d*–spacing at ~32.63 Å, and a broad diffuse peak with a d = ~4.66 Å at wide angle region was obtained. The strong peak with a d = 32.63 Å corresponded to a Miller indices 110 in the

hexagonal columnar arrangement. However, liquid–like correlations between the rigid cores occurred at wide–angle regions of ~4.66 Å. This diffraction pattern corresponded to an intercolumnar distance or lattice constant (i.e., a parameter of the hexagonal lattice) of a = 37.67 Å. The lack of any relatively peaks at wide angles excluded a more regular periodicity along the columns.

Columnar mesogens were characterized by columns of molecules, and within the columns all molecules were packed together to form a two–dimensional crystalline array. On the other hand, for compound **1b** (n = 12), the diffraction pattern was different; one strong diffraction peak and one much weaker peak at lower angle, and one broad diffused peak at wide–angle were observed. The *d*–spacings occurred at *d* = 37.85 Å and 19.11 Å and a broad diffused peak at 4.60 Å. This type of diffraction pattern corresponded to lamellar phases (Col_L) with Miller indices 001 and 002. Higher diffraction peaks indexed as 003, and others were not observed in this discotic system.

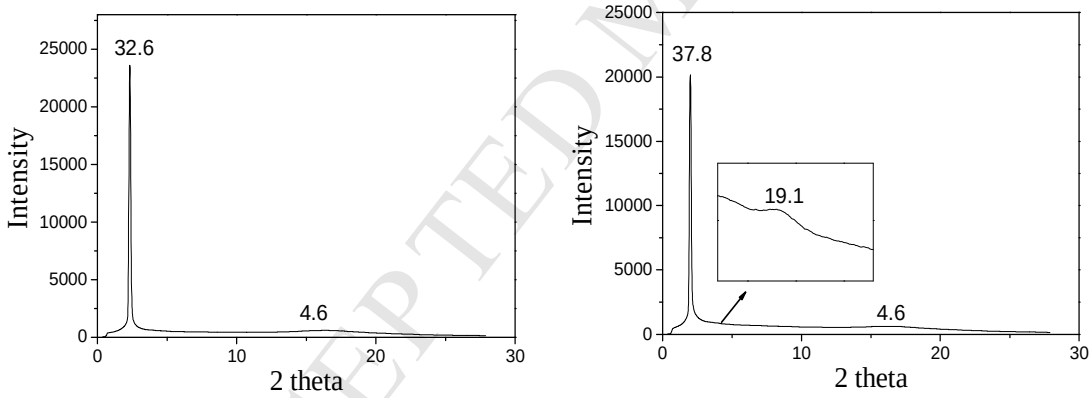

Fig. **4** The powder X–ray diffraction plots of compound **1a** (n = 12; left) measured at 120.0 ^{o}C and **1b** (n = 12; right) measured at 105.0 ^{o}C when cooled from above their clearing temperatures.

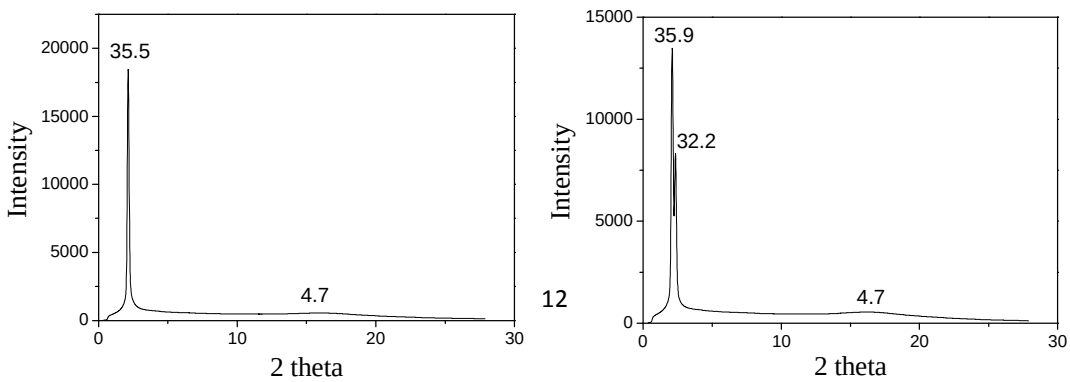

Fig. 5 The powder X–ray diffraction plots of compound **1d** (n = 12; left) measured at 150.0 ^{o}C and **1d** (n = 12; right) measured at 125.0 ^{o}C when cooled from above their clearing temperatures.

Interestingly, compound **1d** (n = 12) showed a different columnar behavior; rectangular columnar phases at lower temperature (T = 125.0 °C) and hexagonal columnar phases at higher temperature (T = 150.0 °C). This compound showed a diffraction pattern of two strong peaks with a *d*–spacing of ~35.87 and ~32.21Å at 125 °C, and these two strong peaks corresponded to Miller index 110 and 210. The rectangular columnar mesophases includes three different Col_{rec} mesophases depending on the planar space groups, P21/a, P2/a, and C2/m, which corresponded to the plane groups p2gg, p2mg, and c2mm, respectively. The exact Col_{rec} was not possible to identify in this example due to its lesser diffraction peaks. In general, the molecules in Col_{rec} phases were tilted with respect to the column axis, leading to an elliptic cross section of the column. As the cross section of the tilted columns is elliptical, the symmetries of the Col_r phases differ from a proper hexagonal symmetry.

The formation of discotic or columnar mesophases by round or discotic molecules was often strongly side chain dependent. More side chains are generally needed for larger core centers in order to stabilize the mesogen. A phase crossover between rectangular and hexagonal columnar phases was in fact observed for compound **1d** (n =12), as shown in Fig. 5. A phase crossover between Col_{hex} and Col_r phases was less observed, and these phase transitions were often related or dependent to the temperature or/and side chain length of compounds. The mesophase crossover[12] from Col_{rec} to Col_{hex} has been observed in columnar systems, and was generally attributed to the greater core interaction necessary for the formation of the Col_r phases. The tilted Col_r phase reduced the interactions between the bulky side chains and allowed closer contacts between the cores. This pseudohexagonal lattice constant (*i.e*. a rectangular lattice with an axial ratio of *b/a* from the ideal hexagonal of √3; Fig. 6) for this series of compound **1d** (n = 12) was

equal to 1.49 (*i.e*. 64.42/43.19). This valve indicated that the structural departure from the ideal hexagonal lattice was about 33.0% in this system. A summary of the diffraction peaks and lattice for these three compounds **1a**–**b** and **1d** (all n = 12) is listed in Table 3.

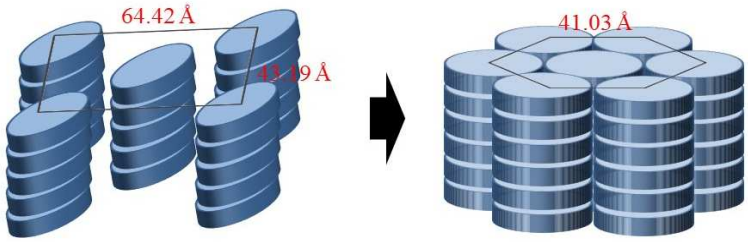

Fig. 6 The structural departure from the ideal hexagonal lattice in compounds **1d** (n = 12)

Table 3. Detailed indexation by powder XRD of columnar phases[a] for compounds **1a, 1b, 1d**

Compds.	Mesophases temp.	*d*-Spacing obs.(calcd.)	Lattice const. (Å)	Miller Indices
1a (n = 12)	Col_h at 120.0°C	32.63 (32.63)	*a* = 37.67	100
		4.66 (br)		halo
1b (n = 12)	Col_L at 105.0°C	37.85 (37.85)		100
		19.11 (18.93)		200
		4.60 (br)		halo
1d (n = 12)	Col_h at 150.0°C	35.54 (35.54)	*a* = 41.03	100
		4.72 (br)		halo
1d (n = 12)	Col_r at 125.0 °C	35.87 (35.87)	*a* = 64.42	110
		32.21 (32.21)	*b* = 43.19	200
		4.66 (br)		halo

[a]: temperature taken on the cooling process;

In order to understand the possible molecular packing in the columnar phases, the number of molecules within a portion of columnar height *h* was calculated by use of a known model.[13] By this simple model, two important parameters; N_{cell} and R_{ar} were then calculated from powder X–ray diffraction data. N_{cell} is the number of molecules within a 9.0 Å column, and the R_{ar} defined as the diameter of the aromatic or hard columnar part was calculated by $R_{ar} = (4S_{ar}/\pi)^{1/2}$. A value of N_{cell} = 2.85 and 2.16 was obtained for compounds **1a** (n = 12) at 120 °C and **1d** (n = 12) at 150

°C. On the other hand, an average number of ca. 2.16–2.85 molecules for compounds **1a** or **1d** were stacked within a height of 9.0 Å in the columnar phases (Table 4). Therefore, a more disc-like correlated structure constructed by two molecules lying up–and–down was generated within the column. The possible molecular arrangement in columnar phases was proposed in Fig. 7 and Fig. 8.

Table 4. Geometric parameters[a] of compound **1a** (n = 12) and **1d** (n = 12).

Compd.	S(Å^2)	V_{cell}(Å^3)	V_m(Å^3)	Temp(°C)	N_{cell}	S_{ar}(Å^2)	R_{ar}(Å)
1a (n = 12)	1228.68	11058.08	3873.83	120.0	2.85	329.86	20.49
1d (n = 12)	1457.67	13119.05	6069.02	150.0	2.16	406.14	22.74

[a]: S(Å^2) = columnar cross section area, V_{cell}(Å^3) = volume of the column stratum 9 Å thick, V_m(Å^3) = molecular volume, N_{cell} = the number of molecules contained in each columnar stratum 9–Å thick, S_{ar}(Å^2) = the surface area of hard columnar core, R_{ar} (Å^2) = the diameter of the aromatic part.

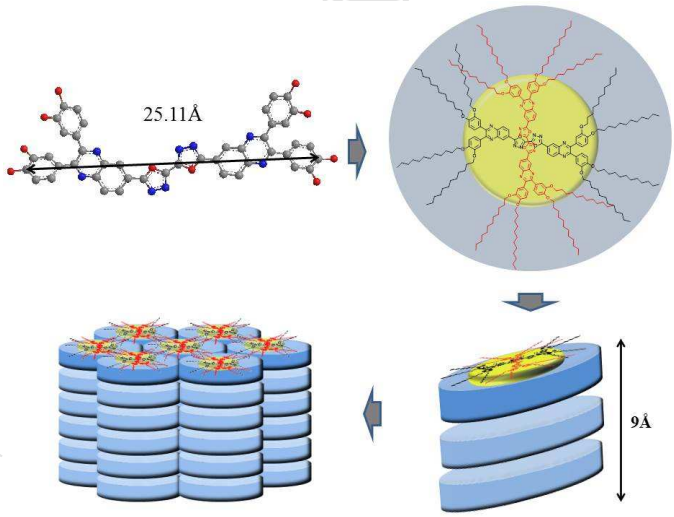

Fig. 7 A schematic representation of molecular organization proposed in columnar phase by compounds **1a**.

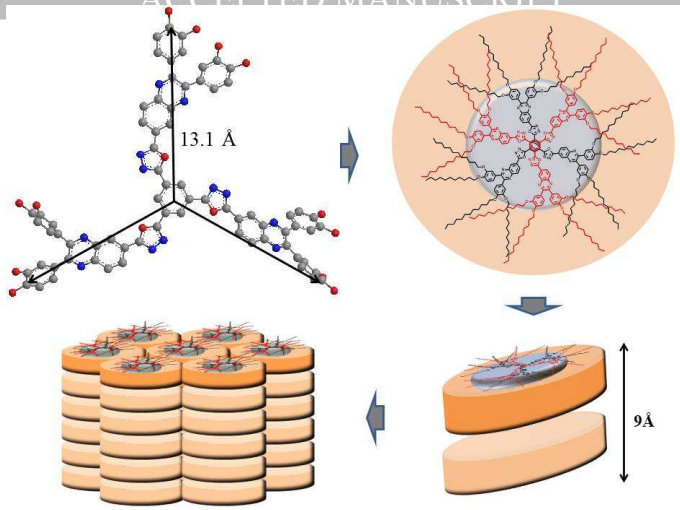

Fig. 8 A schematic representation of molecular organization proposed in columnar phase by compounds **1d**.

2.4 Optical properties

1,3,4–Oxadiazole has been long known to be an excellent blue-emitter and has potential applications in OLED devices. The UV–vis absorption and PL spectra of the compounds **1a–d** (all n = 12) excited at λ = 342 cm^{-1} measured in CH_2Cl_2 solution at room temperature are presented in Fig. 9 and data presented in Table 5. These compounds containing bis– and tris–1,3,4–oxadiazoles are particularly interesting due to the presence of multiple chromophores and possible π–conjugations between the peripheral structures and central core. The absorption λ_{max} peaks of compounds **1a–d** occurred at ca. ~342 and 403–410 nm, which were attributed to π–π* transitions, arising from 1,3,4–oxadiazole and quinoxaline, respectively. Compound **1a** (n = 12) has a slightly red–shifted λ_{max} than those of others, which might be due to its better coplanar core. Single crystallographic data[14] of similar 1,3,4–oxadiazoles have indicated that a dihedral angle between the benzene and 1,3,4–oxadiazole was often ranged of ~ 0–15.5°.In contrast, the PL spectra of all compounds **1a–d** showed one intense and broad peak occurred at λ_{max} = 517–529 nm, respectively, and these photo luminescent emissions originated from quinoxaline moieties, similar to our previous systems containing 1,3,4-oxaziazole and/or quinoxalinez. The λ_{max} in compounds **1a** and **1d** are slightly red–shifted due to their better conjugation lengths. In general, a red-shift emission

is often expected in this type of conjugated systems. All three *bis*-1,3,4-oxadiazoles **1a**–**c** have a much red–shifted λ_{max} = 517–529 nm than those of our previous studied bis–1,3,4–oxadiazole, 2,5-bis(5-(3,4,5-tris (dodecyloxy)phenyl)- 1,3,4-oxadiazol-2-yl)thiophene and others. An apparent red–shifted λ_{max} in this system than those of 1,3,4-oxadiazoles might be attributed to the more electron–donating group of peripheral quinoxalines. All quantum yields of luminescent materials were ranged from 30 to 35%. However, an emission often seen by 1,3,4–oxadiazoles at ca. 380–418 nm was not observed. Both quinoxaline and 1,3,4–oxadiazoles were considered as π–acceptors and fluorophore, and a red–shift emission often attributed to donor–acceptor transfer. Whether a fluorescence resonance energy transfer (FRET) involved in this system was uncertain at this moment, and more experimental data might be needed. FRET states a mechanism in which the resonance energy transfers from an excited state of a donor fluorophore to the ground state of an acceptor fluorophore via a non-radiative 'dipole-dipole coupling'. In order to have this photo effect, both fluorescent chromophores need to be within a certain distance,

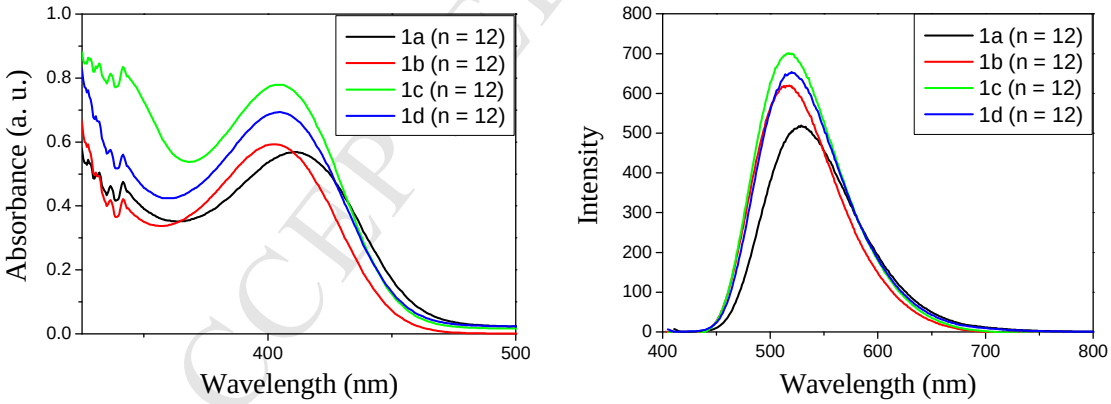

Fig. 9 Absorption (left), and PL spectra (right) of the compounds **1a**–**d**.

Table 5. The UV−*vis* absorption and PL−emission data[a] of compounds **1a–1d**.

Compds	Absorption λ (nm)	Emission[b] λ_{max} (nm)	Φ_F
1a (n = 12)	342, 410	529	0.33
1b (n = 12)	342, 403	518	0.35
1c (n = 12)	342, 405	517	0.30
1d (n = 12)	342, 405	520	0.33

[a]: All data measured in CH_2Cl_2 at room temperature. Anthracene is used as standard with a Φf_s = 0.27 in hexane solution.

[b]: the excitation wavelength is 342 cm^{-1}.

3. Conclusions

Quinoxaline moieties was incorporated into bis-(1,3,4-oxadiazoles) **1a–b** and tris−(1,3,4−oxadiazoles) **1d** to better induce their columnar phases. The formation of columnar phases was sensitive to the molecular conformations. Compounds **1a** (n = 8, 12) formed Col_h phases, while compounds **1b** (n = 12) exhibited Col_L phases. In contrast, all compound **1d** formed Col_r at lower temperature and Col_h phases at higher temperature. The phase crossover in such a tris-(1,3,4-oxadiazoles) might be attributed to the kinetically unstable conformations resulted from the bulky quinoxalines pendant around the central core. The PL spectra of all compounds **1a–d** showed one intense peak at λ_{max} = 517−520 nm, which was originating from the fused quinoxaline. The lack of blue emissions at ca. λ_{max} = 390−418 nm by 1,3,4−oxadiazoles might be probably due to the effect of fluorescence resonance energy transfer.

4.0 Experimental Section

4.1. General materials and methods

All chemicals and solvents were reagent grade from Aldrich Chemical Co., and solvents were dried by standard techniques. ^1H and ^{13}C NMR spectra were measured on a Bruker DRS-300. DSC thermographs were carried out on a Mettler DSC−822 and calibrated with a pure indium sample. All phase transitions are determined by a scan rate of 10.0 °C/min. Optical polarized microscopy was carried out on Zeiss Axioplan two equipped with a hot stage system of Mettler

FP90/FP82HT. The UV−vis absorption and fluorescence spectra were obtained using a Jasco V−530 and Hitachi F−4500 spectrometer. Elemental analyses were performed on a Heraeus CHN−Rapid elemental analyzer. The powder diffraction data were collected from the Wiggle A beam line of the National Synchrotron Radiation Research Center (NSRRC) with a wavelength of 1.3223 Å. The powder samples were charged in Lindeman capillary tubes (80 mm long x 0.01 mm thick) purchased from Charles Supper Co. with an inner diameter of 1.0 mm.

4.2 1, 2–Bis(dodecyloxy)benzene

^{1}H NMR (300 MHz, $CDCl_3$): δ 0.85 (t, 6H, $–CH_3$, *J* = 6.9 Hz), 1.24–1.45 (m, 36H, $–CH_2$), 1.74–1.84 (m, 4H, $–CH_2$), 3.97 (t, 4H, $–OCH_2$, *J* = 6.6 Hz), 6.86 (s, Ar–H, 4H). ^{13}C NMR (75 MHz, $CDCl_3$): δ 14.14, 22.72, 26.07, 29.38, 29.47, 29.67, 29.73, 31.95, 69.29, 114.12, 121.00, 149.25.

4.3 1, 2–Bis(3,4–bis(dodecyloxy)phenyl)–1, 2–ethanedione 5 (n = 12)

^{1}H NMR (300 MHz, $CDCl_3$): δ 0.83–0.88 (m, 12H, $–CH_3$), 1.24–1.45 (m, 72H, $–CH_2$), 1.77–1.86 (m, 8H, $–CH_2$), 4.01–4.05 (m, 8H, $–OCH_2$), 6.81 (d, 2H, Ar–H, *J* = 8.4 Hz), 7.39–7.42 (m, 2H, Ar–H), 7.54 (d, 2H, Ar–H, *J* = 1.8 Hz). ^{13}C NMR (75 MHz, $CDCl_3$): δ 14.14, 22.72, 25.94, 26.00, 28.93, 29.08, 29.40, 29.66, 31.95, 69.11, 69.22, 111.54, 112.19, 126.17, 149.29, 154.97, 193.83.

4.4 Methyl 2,3–bis(3,4–bis(dodecyloxy)phenyl)quinoxaline–6–carboxylate 4 (n = 12)

The solution 1, 2–bis(3, 4–bis(dodecyloxy)phenyl)–1, 2–ethanedione (4.0 g, 4.0 mmol) dissolved in 100 mL of THF was stirred with 0.5 mL of glacial acetic acid for 10 min. To the solution, methyl 3,4–diaminobenzoate (0.70 g, 4.0 mmol) was added and stirred for 24 h. The product, isolated as yellow solids was obtained after recrystallization from THF/MeOH. Yield 93%, ^{1}H NMR (300 MHz, $CDCl_3$): δ 0.86 (t, 12H, $–CH_3$, J = 6.6 Hz), 1.25–1.42 (m, 72H, $–CH_2$), 1.68–1.83 (m, 8H, $–CH_2$), 3.80–3.81 (m, 4H, $–OCH_2$), 3.98–4.00 (m, 7H, $–OCH_2$, $–OCH_3$), 6.82 (d, 2H, Ar–H, *J* = 8.4 Hz), 7.07–7.15 (m, 4H, Ar–H), 8.12 (d, 1H, Ar–H, *J* = 8.7 Hz), 8.28 (d, 1H, Ar–H, *J* = 8.4 Hz), 8.82 (s, 1H, Ar–H). 13C NMR (75 MHz, CDCl3): δ 14.05, 22.64, 25.99, 29.11, 29.19, 29.34, 29.39, 29.64, 31.89, 52.42, 69.15, 113.09, 115.30, 122.84, 122.96, 128.96, 129.11, 130.67, 131.31, 131.67, 140.12, 142.96, 148.72, 150.13, 150.26, 154.07, 154.78, 166.39.

4.5 2,3–Bis(3,4–bis(dodecyloxy)phenyl)quinoxaline–6–carbohydrazide 3 (n = 12)

The solution of methyl 2,3–bis(3,4–bis(dodecyloxy)phenyl)quinoxaline–6–carboxylate (4.0 g, 4.0 mmol) dissolved in 100 mL of THF and 50 mL of methanol. To the solution, hydrazine monohydrate (2 g, 40.0 mmol) was added and stirred for 12 h. The product, isolated as yellow solids was obtained after recrystallization from THF/MeOH. Yield 90%, 1H NMR (300 MHz, CDCl3): δ 0.85 (t, 12H, $-CH_3$, *J* = 6.3 Hz), 1.24–1.42 (m, 72H, $-CH_2$), 1.68–1.81 (m, 8H, $-CH_2$), 3.78 (m, 4H, $-OCH_2$), 3.97 (m, 4H, $-OCH_2$), 4.23 (s, 2H, $-NH_2$), 6.84 (d, 2H, Ar–H, *J* = 8.4 Hz), 7.03 (d, 2H, Ar–H, *J* = 6.3 Hz), 7.09 (d, 2H, Ar–H, *J* = 8.1 Hz), 8.09 (s, 2H, Ar–H), 8.42 (s, 1H, Ar–H). ^{13}C NMR (75 MHz, $CDCl_3$): δ 14.06, 22.65, 26.00, 29.12, 29.20, 29.34, 29.42, 29.66, 31.89, 69.19, 113.06, 115.30, 122.83, 122.95, 127.59, 129.61, 131.20, 133.20, 140.10, 142.33, 148.70, 150.18, 150.26, 154.16, 154.58, 167.80.

4.6 N'1,N'2–Bis(2,3–bis(3,4–bis(dodecyloxy)phenyl)quinoxaline–6–carbonyl)oxalohydrazide 2a (n = 12)

The solution of 2,3–bis(3,4–bis(dodecyloxy)phenyl)quinoxaline–6–carbohydrazide (1.0 g, 1.0 mmol) dissolved in 125 mL of THF was added dropwise 0.14 mL of triethylamine (1.0 mmol) at ice bath. Oxalyl chloride (0.03 g, 0.5 mmol) was slowly added to the solution and stirred at r.t. for 24 h. The solution was concentrated to give yellow–green solids. The solids were dissolved in 150 mL of dichloromethane and extracted with 100 mL of water. The resulting crude product **2a** was directly used for next reaction. All other three compounds **2b–d** were similarly prepared as above procedures.

4.7 5,5'–Bis(2,3–bis(3,4–bis(dodecyloxy)phenyl)quinoxalin–6–yl)–2,2'–bi(1,3,4–oxadiazole) 1a (n = 12)

The solution of crude product N'1,N'2–bis(2,3–bis(3,4–bis(dodecyloxy)phenyl)quinoxaline–6–carbonyl)oxalohydrazide (1.0 g, 4.0 mmol) dissolved in 20 mL of phosphoryl chloride was refluxed for 24 h. The solution slowly turned reddish-black in color. The solution was cooled at room temperature, and then the solution was slowly poured into 300 mL of icy water. After stirring for 2 h, the orange solids were filtered and collected. The solids were dissolved in 150 mL of

dichloromethane and extracted with 150 mL of 1.0 M $NaOH_{(aq)}$ for 2 h. The yellow–brown solids were collected. The products isolated as bright yellow solids were obtained after silica gel chromatography eluting with hexane/ethyl acetate and recrystallization from THF/methanol. Yield 25%, mp. 113.6 °C. ^{1}H NMR (300 MHz, $CDCl_3$): δ 0.83–0.88 (m, 24H, $-CH_3$), 1.25–1.42 (m, 144H, $-CH_2$), 1.62–1.84 (m, 16H, $-CH_2$), 3.84 (t, 8H, $-OCH_2$, *J* = 6.6 Hz), 4.00 (t, 8H, $-OCH_2$, *J* = 6.6 Hz), 6.84 (d, 4H, Ar–H, *J* = 8.1 Hz), 7.12–7.19 (m, 8H, Ar–H), 8.27 (d, 2H, Ar–H, *J* = 8.7 Hz), 8.51 (dd, 2H, Ar–H, *J* = 2.1 Hz, *J* = 8.8 Hz), 9.00 (d, 2H, Ar–H, *J* = 1.8 Hz). ^{13}C NMR (75 MHz, $CDCl_3$): δ 14.09, 22.68, 26.04, 29.16, 29.22, 29.37, 29.45, 29.69, 31.92, 69.23, 113.07, 115.26, 122.85, 123.06, 127.00, 129.36, 130.52, 131.02, 131.11, 140.54, 142.82, 148.79, 150.38, 150.48, 153.29, 154.68, 155.14, 165.93. IR (KBr): 2955, 2921, 2850, 2363, 2329, 1600, 1578, 1560, 1541, 1514, 1466, 1423, 1390, 1351, 1423, 1390, 1350, 1423, 1389, 1265, 1252, 1225, 1186, 1142, 1066, 1028, 1003, 932, 889, 817, 727, 627, 488 cm^{-1}. Anal. Calcd for $C_{140}H_{218}N_8O_{10}$: C, 77.37; H, 10.11; N, 5.16. Found C, 77.23; H, 10.11; N, 5.06.

4.7.1 5,5'–Bis(2,3–bis(3,4–bis(octyloxy)phenyl)quinoxalin–6–yl)–2,2'–bi(1,3,4–oxadiazole) 1a (n = 8)

Mp. 134.3 °C; ^{1}H NMR (300 MHz, $CDCl_3$): δ 0.85–0.89 (m, 24H, $-CH_3$), 1.28–1.43 (m, 80H, $-CH_2$), 1.64–1.84 (m, 16H, $-CH_2$), 3.84 (t, 8H, $-OCH_2$, *J* = 6.9 Hz), 4.00 (t, 8H, $-OCH_2$, *J* = 6.6 Hz), 6.84 (d, 4H, Ar–H, *J* = 8.4 Hz), 7.12–7.19 (m, 8H, Ar–H), 8.27 (d, 2H, Ar–H, *J* = 8.7 Hz), 8.51 (dd, 2H, Ar–H, *J* = 1.8 Hz, *J* = 8.7 Hz), 9.00 (d, 2H, Ar–H, *J* = 2.1 Hz). ^{13}C NMR (75 MHz, $CDCl_3$): δ 14.07, 22.66, 26.01, 29.20, 29.26, 29.31, 29.37, 31.82, 69.17, 69.22, 113.05, 115.24, 122.84, 123.05, 126.99, 129.34, 130.50, 131.01, 131.10, 140.53, 142.81, 148.78, 150.36, 150.47, 153.28, 154.67, 155.12, 165.91. IR (KBr): 2957, 2921, 2854, 2364, 1598, 1560, 1514, 1469, 1424, 1394, 1347, 1308, 1260, 1186, 1136, 1068, 1024, 970, 929, 897, 858, 839, 815, 727, 671, 628, 420 cm^{-1}. Anal. Calcd for $C_{108}H_{154}N_8O_{10}$: C, 75.22; H, 9.00; N, 6.50. Found C, 75.22; H, 9.08; N, 6.41.

4.8 1,3–Bis(5–(2,3–bis(3,4–bis(dodecyloxy)phenyl)quinoxalin–6–yl)–1,3,4–oxadiazol–2–yl)benzene 1b (n = 12)

Mp. 93.3 °C. ^{1}H NMR (300 MHz, $CDCl_3$): δ 0.83–0.87 (m, 24H, $-CH_3$), 1.24–1.42 (m, 144H,

–CH_2), 1.68–1.83 (m, 16H, –CH_2), 3.83 (t, 8H, –OCH_2, *J* = 6.6 Hz), 3.99 (t, 8H, –OCH_2, *J* = 6.6 Hz), 6.84 (d, 4H, Ar–H, *J* = 8.4 Hz), 7.10 (d, 4H, Ar–H, *J* = 1.8 Hz), 7.16 (d, 4H, Ar–H, *J* = 8.4 Hz), 7.77 (t, 1H, Ar–H, *J* = 8.1 Hz), 8.26 (d, 2H, Ar–H, *J* = 8.7 Hz), 8.38 (d, 2H, Ar–H, *J* = 7.5 Hz), 8.51 (d, 2H, Ar–H, *J* = 8.7 Hz), 8.91 (s, 2H, Ar–H), 8.98 (s, 1H, Ar–H). ^{13}C NMR (75 MHz, $CDCl_3$): δ 14.07, 22.66, 26.03, 29.16, 29.22, 29.36, 29.45, 29.68, 31.91, 69.21, 113.10, 115.29, 123.02, 124.13, 125.04, 125.23, 127.03, 128.15, 130.01, 130.28, 131.20, 140.59, 142.44, 148.76, 150.26, 150.35, 154.50, 154.71, 164.04, 164.57. IR (KBr): 2922, 2852, 2362, 2329, 1600, 1559, 1509, 1467, 1424, 1394, 1347, 1298, 1261, 1185, 1138, 1068, 1013, 976, 857, 840, 812, 765, 727, 700, 680, 627, 591, 522,501, 485, 469, 462, 447, 437, 417 cm^{-1}. Anal. Calcd for $C_{146}H_{222}N_8O_{10}$: C, 77.96; H, 9.95; N, 4.98. Found C, 77.87; H, 9.95; N, 4.97.

4.9 1,4–Bis(5–(2,3–bis(3,4–bis(dodecyloxy)phenyl)quinoxalin–6–yl)–1,3,4–oxadiazol–2–yl)benzene 1c (n = 12)

Mp. 157.8 °C. ^{1}H NMR (300 MHz, $CDCl_3$): δ 0.84–0.88 (m, 24H, –CH_3), 1.25–1.41 (m, 144H, –CH_2), 1.65–1.82 (m, 16H, –CH_2), 3.83 (q, 8H, –OCH_2, *J* = 4.8 Hz), 4.00 (t, 8H, –OCH_2, *J* = 3.6 Hz), 6.82–6.87 (m, 4H, Ar–H, *J* = 8.4 Hz), 7.08–7.10 (m, 4H, Ar–H), 7.13–7.18 (m, 4H, Ar–H), 8.25 (d, 2H, Ar–H, *J* = 8.7 Hz), 8.38 (s, 4H, Ar–H), 8.50 (dd, 2H, Ar–H, *J* = 2.1 Hz, *J* = 8.7 Hz), 8.88 (d, 2H, Ar–H, *J* = 1.8 Hz). ^{13}C NMR (75 MHz, $CDCl_3$): δ 14.08, 22.68, 26.04, 29.16, 29.23, 29.37, 29.45, 29.69, 31.92, 69.24, 113.14, 115.32, 122.90, 123.05, 124.12, 126.65, 127.02, 127.71, 128.12, 130.31, 131.16, 131.23, 140.60, 142.51, 148.77, 150.30, 150.39, 154.57, 154.78, 164.14, 164.56. IR (KBr): 2921, 2851, 2360, 2340, 1600, 1578, 1561, 1516, 1466, 1304, 1262, 1185, 1139, 1063, 1013, 894, 850, 816, 728, 688, 669, 629, 518, 488, 401 cm^{-1}. Anal. Calcd for $C_{146}H_{222}N_8O_{10}$: C, 77.96; H, 9.95; N, 4.98. Found C, 77.71; H, 9.97; N, 4.93.

4.10 1,3,5–Tris(5–(2,3–bis(3,4–bis(octyloxy)phenyl)quinoxalin–6–yl)–1,3,4–oxadiazol–2–yl)benzene 1d (n = 8)

Mp. 102.0 °C. ^{1}H NMR (300 MHz, $CDCl_3$): δ 0.85–0.89 (m, 24H, –CH_3), 1.28–1.43 (m, 80H, –CH_2), 1.64–1.84 (m, 16H, –CH_2), 3.84 (t, 8H, –OCH_2, *J* = 6.9 Hz), 4.00 (t, 8H, –OCH_2, *J* = 6.6 Hz), 6.84 (d, 4H, Ar–H, *J* = 8.4 Hz), 7.12–7.19 (m, 8H, Ar–H), 8.27 (d, 2H, Ar–H, *J* = 8.7 Hz),

8.51 (dd, 2H, Ar–H, *J* = 1.8 Hz, *J* = 8.7 Hz), 9.00 (d, 2H, Ar–H, *J* = 2.1 Hz). ^{13}C NMR (75 MHz, $CDCl_3$): δ 14.07, 22.66, 26.01, 29.20, 29.26, 29.31, 29.37, 31.82, 69.17, 69.22, 113.05, 115.24, 122.84, 123.05, 126.99, 129.34, 130.50, 131.01, 131.10, 140.53, 142.81, 148.78, 150.36, 150.47, 153.28, 154.67, 155.12, 165.91. IR (KBr): 3072, 2926,2 853, 2581, 2366, 1733, 1598, 1514, 1467, 1423, 1392, 1346, 1297, 1261, 1186, 1136, 1068, 1022, 971, 933, 896, 863, 841, 809, 780, 730, 675, 628, 485, 423 cm^{-1}. Anal. Calcd for $C_{168}H_{234}N_{12}O_{15}$: C, 75.81; H, 8.86; N, 6.31. Found C, 74.81; H, 8.83; N, 6.10.

4.10.1 1,3,5–Tris(5–(2,3–bis(3,4–bis(decyloxy)phenyl)quinoxalin–6–yl)–1,3,4–oxadiazol–2–yl)benzene 1d (n = 10)

Mp. 104.0 °C. ^{1}H NMR (300 MHz, $CDCl_3$): δ 0.84–0.88 (m, 36H, –CH_3), 1.26–1.43 (m, 168H, –CH_2), 1.71–1.84 (m, 24H, –CH_2), 3.83 (t, 12H, –OCH_2, *J* = 6.3 Hz), 3.99 (t, 12H, –OCH_2, *J* = 6.3 Hz), 6.84 (d, 6H, Ar–H, *J* = 8.1 Hz), 7.12 (s, 6H, Ar–H), 7.15–7.20 (m, 6H, Ar–H), 8.29 (d, 3H, Ar–H, *J* = 8.7 Hz), 8.55 (d, 3H, Ar–H, *J* = 9 Hz), 8.98 (s, 3H, Ar–H) , 9.14 (s, 3H, Ar–H). ^{13}C NMR (75 MHz, $CDCl_3$): δ 14.07, 22.67, 26.03, 29.16, 29.23, 29.38, 29.44, 29.62, 29.68, 31.91, 69.22, 113.07, 115.28, 123.03, 123.82, 126.30, 127.03, 127.58, 128.49, 130.37, 131.10, 131.22, 140.60, 142.52, 148.76, 150.30, 150.37, 154.54, 154.82, 163.20, 165.07. IR (KBr): 3076, 2955, 2922, 2853, 2361, 1600, 1510, 1466, 1423, 1395, 1347, 1261, 1186, 1137, 1069, 1016, 982, 897, 840, 810, 781, 730, 674, 629, 488, 419 cm^{-1}. Anal. Calcd for $C_{192}H_{282}N_{12}O_{15}$: C, 76.91; H, 9.48; N, 5.61. Found C, 76.52; H, 9.59; N, 5.50.

4.10.1 1,3,5–Tris(5–(2,3–bis(3,4–bis(dodecyloxy)phenyl)quinoxalin–6–yl)–1,3,4–oxadiazol–2–yl)benzene 1d (n = 12)

Mp. 110.0 °C. ^{1}H NMR (300 MHz, $CDCl_3$): δ 0.84 (t, 36H, –CH_3, *J* = 6.3 Hz), 1.25–1.43 (m, 216H, –CH_2), 1.69–1.84 (m, 24H, –CH_2), 3.83 (t, 12H, –OCH_2, *J* = 6.3 Hz), 4.00 (t, 12H, –OCH_2, *J* = 6.3 Hz), 6.84 (d, 6H, Ar–H, *J* = 8.4 Hz), 7.12 (s, 6H, Ar–H), 7.15–7.20 (m, 6H, Ar–H), 8.30 (d, 3H, Ar–H, *J* = 8.7 Hz), 8.55 (d, 3H, Ar–H, *J* = 8.7 Hz), 8.98 (s, 3H, Ar–H) , 9.17 (s, 3H, Ar–H). ^{13}C NMR (75 MHz, $CDCl_3$): δ 14.08, 22.67, 26.04, 29.17, 29.23, 29.37, 29.46, 29.69, 31.92, 69.22, 113.07, 115.29, 123.03, 123.83, 126.30, 127.02, 127.58, 128.49, 130.38, 131.10,

131.23, 140.61, 142.52, 148.77, 150.30, 150.38, 154.53, 154.81, 163.20, 165.07. IR (KBr): 3076, 2923, 2544, 2363, 2329, 1602, 1510, 1467, 1424, 1394, 1347, 1261, 1186, 1136, 1071, 1017, 979, 897,841, 809, 730, 677, 628, 440, 413 cm^{-1}. Anal. Calcd for $C_{216}H_{330}N_{12}O_{15}$: C, 77.79; H, 9.97; N, 5.04. Found C, 77.46; H, 9.96; N, 4.98.

4.10.2 1,3,5–Tris(5–(2,3–bis(3,4-bis(tetradecyloxy)phenyl)quinoxalin–6–yl)–1,3,4–oxadiazol–2–yl)benzene 1d (n = 14)

Mp. 115.0 °C. ^{1}H NMR (300 MHz, $CDCl_3$): δ 0.83–0.88 (m, 36H, $–CH_3$), 1.24–1.41 (m, 264H, $–CH_2$), 1.67–1.84 (m, 24H, $–CH_2$), 3.84 (t, 12H, $–OCH_2$, *J* = 6.3 Hz), 4.00 (t, 12H, $–OCH_2$, *J* = 6.6 Hz), 6.84 (d, 6H, Ar–H, *J* = 8.4 Hz), 7.12 (s, 6H, Ar–H), 7.15–7.21 (m, 6H, Ar–H), 8.30 (d, 3H, Ar–H, *J* = 8.7 Hz), 8.56 (d, 3H, Ar–H, *J* = 7.8 Hz), 8.99 (s, 3H, Ar–H) , 9.17 (s, 3H, Ar–H). ^{13}C NMR (75 MHz, $CDCl_3$): δ 14.08, 22.67, 26.05, 29.17, 29.25, 29.36, 29.47, 29.72, 31.92, 69.22, 113.08, 115.29, 123.04, 123.83, 126.36, 127.04, 127.61, 128.50, 130.39, 131.11, 131.24, 140.62, 142.54, 148.78, 150.31, 150.38, 154.56, 154.83, 163.22, 165.10. IR (KBr): 3080, 2922, 2853, 2361, 1599, 1518, 1468, 1424, 1396, 1346, 1261, 1186, 1136, 1026, 897, 810, 730, 419 cm^{-1}. Anal. Calcd for $C_{240}H_{378}N_{12}O_{15}$: C, 78.51; H, 10.38; N, 4.58. Found C, 78.27; H, 10.38; N, 4.53.

Acknowledgements

We thank the Ministry of Science and Technology, Taiwan, ROC (MOST 104–2119–M–008–011) in generous support of this work. Also we deeply appreciated Prof. Hwo-Shuenn Sheu for performing powder XRD experiments at the National Synchrotron Radiation Research Center.

References:

1. (a) Wohrle, T.; Wurzbach, I.; Kirres, J.; Kostidou, A.; Kapernaum, N.; Litterscheidt, J. L.; Haenle, J. C.; Staffeld, P.; Baro, A.; Giesselmann, F.; Laschat, S. *Chem. Rev*. **2016**, *116*, 1139–1241; (b) Hu, Y.; Li, C. Y.; Wang, X. M.; Yang, Y. H.; Zhu, H. L. *Chem. Mater*. **2014**, *114*, 5572-5610; (c) Tao, Y.; Yang, C.; Qin, *J. Chem. Soc. Rev.*, **2011**, *40*, 2943–2970; (d) Grimsdale,

A. C.; Chan, K. L.; Martin, R. E.; Jokisz, P. G.; Holmes, A. B. *Chem. Rev.* **2009**, *109*, 897−1091; (e) Lo, S. C.; Bum, P. L. *Chem. Rev*. **2007**, *107*, 1097−1116; (e) Wang, C.; Jung, G. Y.; Hua, Y.; Pearson, C.; Bryce, M. R.; Petty, M. C.; Batsanov, A. S.; Goeta, A. E.; Howard, J. A. K. *Chem. Mater*. **2001**, *13*, 1167−1173.

2. (a) Gutov, O. *Cryst. Growth Des*. **2013**, *13*, 3953−3957; (b) Bostrom, J.; Honger, A.; Linas, A.; Wellner, E.; Plowright, A. T. *J. Med. Chem*. **2012**, *55*, 1817−1830; (c) Zheng, Y.; Batsanov, A. S.; Bryce, M. R. *Inorg. Chem*. **2011**, *50*, 3354−3362; (d) Fang, Y. K.; Liu, C. L.; Yang, G. Y.; Chen, P. C.; Chen, W. C. *Macromolecules* **2011**, *44*, 2604−2612; (e) Guin, S.; Ghosh, T.; Rout, S. K.; Banerjee, A.; Patel, B. *Org. Lett*. **2011**, *13*, 5976−5979.

3. (a) Zafiropoulos, N. A.; Choi, E. J.; Dingemans, T.; Lin, W.; Samulski, E. T. *Chem. Mater*. **2008**, *20*, 3821−3831; (b) Gallardo, H.; Conte, G.; Tuzimoto, P. A.; Behramand, B.; Molin, F.; Eccher, J.; Bechtold, I. H. *Liq. Cryst*. **2012**, *39*, 1099−1111; (c) Picken, S. J.; Dingemans, T. J.; Madsen, L. A.; Francescangeli, O.; Samulski, E. T. *Liq. Cryst*. **2012**, *39*, 19−23; (c) Prajapati, A. K.; Modi, V. *Liq. Cryst*. **2011**, *38*, 191−199.

4. Closs, F.; Siemensmeyer, K.; Frey, T.; Funhoff, D. *Liq. Cryst.* **1993**, *14*, 629−634.

5. (a) Lu, L. Y.; Kuo, H. M.; Sheu, H. S.; Lee, G. H.; Lai, C. K. *Tetrahedron* **2014**, *70*, 5999−6011; (b) Kuo, H. M.; Li, S. Y.; Sheu, H. S.; Lai, C. K. *Tetrahedron* **2012**, *68*, 7331−7337;

6. (a) Liao, C. T.; Wang, Y. J; Huang, C. S.; Sheu, H. S.; Lee, G. H.; Lai, C. K. *Tetrahedron* **2007**, *63*, 12437−12445.

7. (a) Lin, K. T.; Lee, G. H.; Lai, C. K. *Tetrahedron* **2015**, *71*, 4352−4361; (b) Sivadas, A. P.; Kumar, N. S. S.; Prabhu, D. D.; Varghese, S.; Prasad, S. K.; Rao, D. S. S.; Das, S. *J. Am. Chem. Soc*. **2014**, *136*, 5416−5423; (c) Vieira, A. A.; Cavero, E.; omero, P.; Gallardo, H.; Serrano, J. L.; Sierra, T. *J. Mater. Chem. C*. **2014**, *2*, 7029−7038; (d) Yang, X.; Dai, H.; He, Q.; Tang, J.; Cheng, X.; Prehm, M.; Tschierske, C. *Liq. Cryst.* **2013**, *40*, 1028−1034; (e) Han, J. *J. Mater. Chem. C* **2013**, *1*, 7779−7797; (f) Westphal, E.; Prehm, M.; Bechtold, I. H.; Tschierske, C.; Gallardo, H. *J. Mater. Chem*. **2013**, *1*, 8011−8022; (g) Tang, J.; Huang, R.; Gao, H.; Cheng, X.; Prehm, M.; Tschierske, C. *RSC Adv*. **2012**, *2*, 2842−2847; (h) Choi, E. J.; Xu, F.; Son, J. H.; Zin, W. C. *Mol.*

Cryst. Liq. Cryst. **2011**, *551*, 60−68; (i) Choi, E. J.; Xu, F. *Mol. Cryst. Liq. Cryst*. **2010**, *529*, 147−156; (j) Wang, H.; Zhang, F.; Bai, B.; Zhang, P.; Shi, J.; Yu, D.; Zhao, Y.; Wang, Y.; Li, M. *Liq. Cryst*. **2008**, *35*, 905−912; (k) Seo, J.; Kim, S.; Gihm, S. H.; Park, C. R.; Park, S. Y. J. *Mater. Chem*. **2007**, *17*, 5052−5057.

8. (a) Pradhan, B.; Pathak, S. K.; Gupta, R. K.; Gupta, M.; Pal, S. K.; Achalkumar, A. S. *J. Mater. Chem. C*, **2016**, *4*, 6117–6130; (b) Pathak, S. K.; Gupta, R. K.; Nath, S.; Rao, D. S. S.; Prasad, S. K.; Achalkumar, A. S.. *J. Mater. Chem. C* **2015**, *3*, 2940−2952; (c) Girotto, E.; Eccher, J.; Vieira, A. A.; Bechtold, I. H.; Gallardo, H.; *Tetrahedron* **2014**, *70*, 3355–3360; (d) Frizon, T. E.; Dal-Bó, A. G.; Lopez, G.; da Silva Paula, M. M.; da Silva, L. *Liq. Cryst*. **2014**, *41*, 1162−1172; (e) Al–Malki, M. K. S.; Hameed, A. S.; Al-Dujaili, A. H. *Mol. Cryst. Liq. Cryst.*, **2014**, *593*, 34–42; (f) Achalkumar, A. S.; Hiremath, U. S.; Rao, S. D. D.; Prasad, S. K.; Yelamaggad, C. V. *J. Org. Chem.* **2013**, *78*, 527–544; (g) Prabhu, D. D.; Kumar, N. S. S.; Sivadas, A. P.; Varghese, S.; Das, S. *J. Phys. Chem. B* **2012**, *116*, 13071−13080; (h) Barberá, J.; Godoy, M. A.; Hidalgo, P. I.; Parra, M. L.; Ulloa, J. A.; Vergara, J. M. *Liq. Cryst*. **2011**, *38*, 679−688; (i) Varghese, S.; Kumar, N. S. S.; Krishna, A.; Rao, D. S. S.; Prasad, S. K.; Das, S. *Adv. Funct. Mater*. **2009**, *19*, 2064−2073; (j) Yelamaggad, C. V.; Achalkumar, A. S.; Rao, D. S. S.; Prasad, S. K. *J. Org. Chem*. **2009**, *74*, 3168−3171; (k) Cristiano, R.; Pereira, D. M.; Santos, D. O.; Gallardo, H. *Liq. Cryst*. **2005**, *32*, 7−14. (l) Verheyde, B.; dahaen, W. *J. Org. Chem*. **2001**, 66, 4062–4064.

9. (a) Venkateswararao, A.; Tyagi, P.; Thomas, K. R. J.; Chen, P. W.; Ho, K. C. *Tetrahedron* **2014**, *70*, 6318–6327; (b) Gallardo, H.; Ferreira, M.; Vieira, A. A.; Westphal, E.; Molin, F.; Eccher, J.; Bechtold, I. H. *Tetrahedron* **2011**, *67*, 9491−9499; (c) Qu, S.; Li, M. *Tetrahedron* **2007**, *63*, 12429−12436; (d) Zhang, P.; Bai, B.; Wang, H.; Qu, S.; Yu, Z.; Ran, X.; Li, M. *Liq. Cryst*. **2009**, *36*, 7−12.

10. (a) Krzyczkowska, P.; Krówczyński, A.; Kowalewska, J.; Romiszewski, J.; Pociecha, D.; Szydłowska, *J. Mol. Cryst. Liq. Cryst*. **2012**, *558*, 93−101; (b) Velusamy, M.; Huang, J. H.; Hsu, Y. C.; Chou, H. H.; Ho, K. C.;Wu, P. L.; Chang,W. H.; Lin, J. T.; Chu, C. W. *Org. Lett*. **2009**, *11*, 4898–4901.

11. (a) Hu, T. S.; Lin, K. T.; Mu, C. C.; Kuo, H. M.; Chen, M. C.; Lai, C. K. *Tetrahedron* 2014, *70*, 9204–9213; (b) Lin, K. T.; Kuo, H. M.; Sheu, H. S.; Lai, C. K. *Tetrahedron* **2013**, *69*, 9045–9055;

12. (a) Cienega–Cacerez, O.; Moreno–Razo, J. A.; Díaz–Herrera, E.; Sambriski, E. J. *Soft Mater*. **2014**, *10*, 3171–3182; (b) Kumar, S. in "Chemistry of Discotic Liquid Crystals: From Monomers to Polymers", CRC press, Taylor and Francis, **2011**; (c) Wuckert, E.; Hägele, C.; Giesselmann, F.; Baro, A.; Laschat, S. Beil. *J. Org. Chem*. **2009**, 5, 1–7.

13. (a) Ziessel, R.; Pickaert, G.; Camerel, F.; Donnio, B.; Guillon, D.; Cesario, M.; Prange, T. *J. Am. Chem. Soc*. **2004**, *126*, 12403–12413; (b) Donnio, B.; Heinrich, B.; Allouchi, H.; Kain, J.; Diele, S.; Guillon, D.; Bruce, D. W. *J. Am. Chem. Soc.* **2004**, *126*, 15258–15268; (c) Morale, F.; Date, R. W.; Guillon, D.; Bruce, D. W.; Finn, R. L.; Wilson, C.; Blake, A. J.; Schr€oder, M.; Donnio, B. *Chem. Eur. J*. **2003**, *9*, 2484–2501; (d) Attias, A. J.; Cavalli, C.; Donnio, B.; Guillon, D. P.; Hapiot, M. J. *Chem. Mater*. **2002**, *14*, 375–384.

14. (a) Qu, S.; Wang, H.; Zhu, W.; Luo, J.; Fan, Y.; Song, L.; Zhang, H. X.; Liu, X. *J. Mater. Chem.*, **2012**, *22*, 3875–3881; (b) Yang, C. C.; Hsu, C. J.; Chou, P. T.; Cheng, H. C.; Su, Y. O.; Leung, M. K. *J. Phys. Chem. B*, **2010**, *114*, 756–768; (c) Zafiropoulos, N. A.; Choi, E. A.; Ingemans, T.; Lin, W.; Samulski, E. T. *Chem. Mater*, **2008**, *20*, 3821–3831